Research Square

Preprints are preliminary reports that have not undergone peer review.
They should not be considered conclusive, used to inform clinical practice,
or referenced by the media as validated information.

Design Of Earth-Abundant W(0) Complexes For Near-Infrared Absorbance Via Ligand Optimization

Victoria Oas
North Dakota State University
Wenfang Sun
University of Alabama System
Dmitri Kilin
North Dakota State University https://orcid.org/0000-0001-7847-5549
Svetlana Kilina
svetlana.kilina@ndsu.edu

North Dakota State University

Research Article

Keywords:

Posted Date: November 4th, 2026

DOI: https://doi.org/10.21203/rs.3.rs-11600413/v1

License: This work is licensed under a Creative Commons Attribution 4.0 International License.
Read Full License

Additional Declarations: The authors declare no competing interests.

Design Of Earth-Abundant W(0) Complexes For Near-Infrared Absorbance Via Ligand Optimization

Victoria Oas[(1)], Wenfang Sun[(2)], Dmitri Kilin[(1)], and Svetlana Kilina[(1)]

[(1)] Department of Chemistry and Biochemistry, North Dakota State University, Fargo ND 58108

[(2)] Department of Chemistry and Biochemistry, The University of Alabama, Tuscaloosa AL 35487

Abstract:

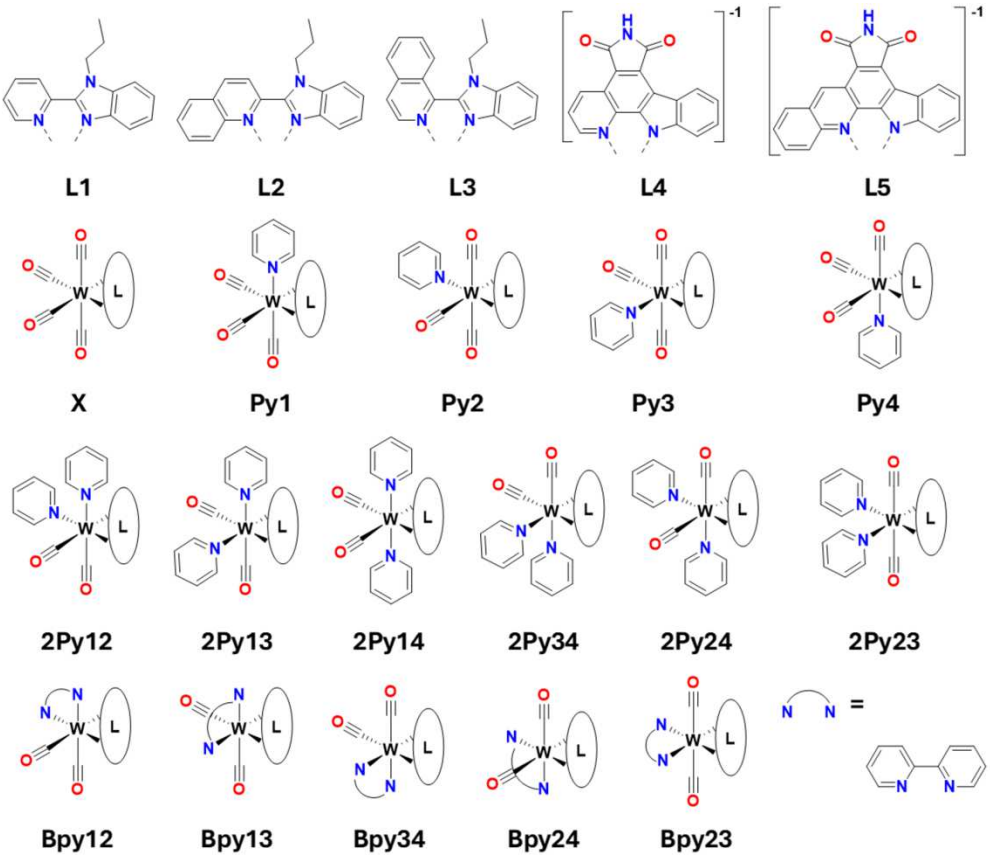
This work focuses on developing new earth-abundant metal complexes to be used as efficient near-infrared (NIR) absorbers and photosensitizers for applications in photocatalysis, bioimaging, and photodynamic therapy. By modifying ligand types coordinated to a W(0) center, we aim to enhance NIR absorption and reduce nonradiative decay pathways in turn. Through collaboration with experimentalists in Dr. Wenfang Sun's group, they were able to synthesize new W(0) complexes coordinated with four carbonyl's and one 2-(pyrid-2-yl)(benz)imidazole ligand. Where it was found that these complexes exhibit strong absorption at 580-600 nm spectral range in dichloromethane. Our calculations based on time-dependent density functional theory (TD-DFT) predict that employing diamine-based ligands with varying conjugation positions or pyridocarbazole-type ligands, can significantly redshift the absorption bands into the NIR region up to 700 nm range. Furthermore, replacing 1-2 of the carbonyl groups with pyridines or bipyridines in these complexes extends the spectra from 500-700 nm up to 800-1100 nm and significantly enhances the optical activity of the lowest energy transitions, indicating promising avenues for efficient emission. It was also found that this overall increase in conjugation on the molecules has increased the amount of mixing in singlet and triplet states in comparison to the 4 carbonyl cases. This indicated promising avenues for efficient inter-system crossing for applications such as photodynamic therapy. Our results demonstrate a promising pathway toward the rational design of W(0) complexes with optical response in the NIR range, advancing the development of cost-effective, earth-abundant NIR emitters for application in photocatalysis, bioimaging and photodynamic therapy.

Introduction:

Transition metal coordinated complexes have been of great interest in recent years due to their optical properties and versatility that allow them to be used in a variety of applications including photovoltaics, photocatalysis and as photosensitizers in photodynamic therapy. Ir(III), Ru(II), and Os(II) complexes have gained attention over the years due to their photophysical and optical properties[1]. These types of complexes however

are made from precious metals that have low abundance in the Earth's crust causing a need to find transition metal complexes that have similar properties but are more earth abundant[2]. Cu(I) complexes have been extensively researched in recent years due to them having similar optical properties as the rare earth metals, but there is still issues that need to be tackled in order to get the desired photophysical properties needed[3]. One earth abundant transition metal that appears to not be extensively studied at this time are tungsten complexes. Tungsten complexes are of great interest due to their displaying of photoluminescence[4,5] and visible absorption that can reach the near IR range[6] with metal to ligand charge transfer transitions.[7] In this work we look into the optical properties of W(0) carbonyl imidazole and carbonyl pyridocarbazole complexes and how the replacement of carbonyl groups with pyridine or bipyridine effects these optical properties in comparison to the four carbonyl versions of these complexes.

Data/Results:



Scheme 1: Shows the computed complexes for all isomer types. X will be labeled based on the attached ligand (ex: 1) and all isomers will be labeled by the attached ligand followed by the isomer type (ex: 1-Py1).

For this work we started by optimizing and comparing complexes 1, 2 and 3 (Scheme 1) absorbance spectrums with those found experimentally through our collaboration with Dr. Wenfang Sun's group (Figure 1a and 1b) to confirm that our methods (see methods section) matched well with experiment before continuing on with similar complexes that have not been synthesized. When we compared the experimental spectra in **Figure 1a** to those computed in **Figure 1b**, the first optically active peak for complexes 1-3 matches with the position of the experimental peak almost exactly for all 3 cases. Where complex 1 is the bluest shifted at ~490 nm, complex 2 is next at ~540 nm and complex 3 is the reddest shifted at ~550 nm. The second peak for these complexes (between 300-400 nm) also seems to match up well with experiment. This shows that our methods match with the trends seen in experiment except for the intensity of the first optically active peak for complex 2; this change in intensity could be caused by the slight twisting in the L2 ligand and rotation of the nPr substituting group. Although the twist and rotation of the substituting group should not affect the position of the peak these slight variations could cause a change in the contribution of the natural transition orbitals (NTO's), as we will discuss at a later point in more detail, that could affect the overall intensity of the peak. Overall, our methods match well with experiment, giving us trust in our predicted results in the rest of the complexes discussed in this paper. These complexes, however, are not absorbed in the NIR range which is needed for applications such as photovoltaics and photodynamic therapy. The first state is also in-optically active, which could affect photoluminescence for these complexes.

A paper published in 2022 by Daniel Álvarez et al on rhenium(I) carbonyl complexes uses a pyridoindole ligand that is extremely similar to L1 discussed in this paper but it is missing the nitrogen attached to the substitution group as well as has a hydrogen instead of a n-propal group[8]. In that paper they show that adding rigidity and steric hindrance to the ligand (complex I-III in the paper) caused a redshift in the absorbance spectra and caused the first state to become optically active[8]. With how close these ligands where to our three complexes we wanted to see if we would get similar results with our W(0) carbonyl complexes; so we replaced our imidazole ligand with their similar pyridocarbazole-type ligand (L4 in **scheme 1**)[8]. What was found that the absorbance spectra was significantly red shift compared to the imidazole ligands (**Figure 1c**). Complex 4's first optically active peak is ~630nm which is almost 100 nm closer to the NIR range compared to complex 3. We also see that with complex 4 the first computed state becomes optically active unlike the imidazole ligands that had the 3rd state being the optically active state. This first state being optically active could mean that this complex would be more photoluminescent than the imidazole ligands, allowing them to be used in more applications including photodynamic therapy. Next, we wanted to see if we would see a further redshift with increased conjugation to complex 4 like what was seen for complexes 1-3 so a benzene ring was added in a similar

position as L2 to create L5 (**scheme 1**). With the increase in conjugation in complex 5 we do see a red shift similar to that of the imidazole complexes (1-3) when compared to complex 4; of roughly 50nm shift with increased conjugation (**Figure 1c**). Similarly, we see that the shift has no effect on changing which state is optically active but instead affects the intensity of the state.

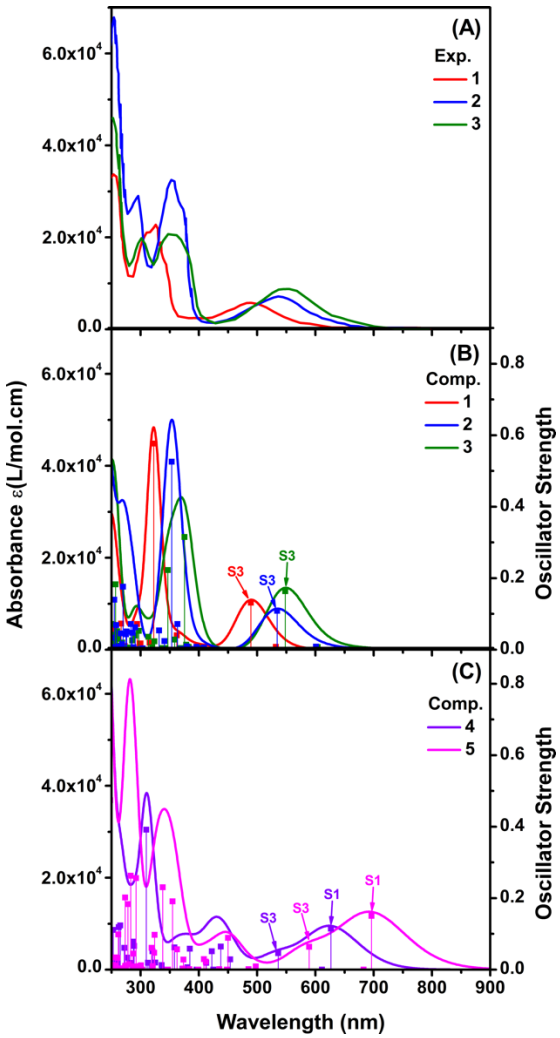


Figure 1: Comparison of absorption spectra obtained from experiment for complex 1, 2, and 3(a) and absorption spectra obtained from calculations for complex 1, 2, and 3 (b) and complex 4 and 5 (c). The state that makes up the first optically active state that is or would be seen experimentally is shown in each corresponding spectrum color (complex 1 [red], 2 [green], 3 [blue], 4 [purple] and 5[magenta]).

After studying the effect of increasing the conjugation and rigidity of the ligand in these complexes, next we wanted to test how adding conjugation to the complex itself by replacing the carbonyl groups with either a pyridine, two pyridines or a bipyridine group

would affect the absorption for all ligand types. Of course, this type of change in the molecules leads to isomers to form from the pyridines and bipyridines attaching to the molecule in different ways (**Scheme 1**). The formation of a variety of isomers called for an analysis of the difference in total energies of each isomer to determine if there were any isomers that are significantly energetically favorable over others. In **Figure 2** we show the results from this comparison of energy differences. What was found was that in all complexes with one pyridine attached (**Figure 2a**) Py1 is the most energetically favorable isomer. In the cases when L4 and L5 are the ligand attached, there is insignificant energy change between Py1 and Py4 due to the planarity of the ligand. Whereas L1-L3 have an increasing amount of twisting in the ligand causing it so each axial positions are increasingly energetically different as the twisting increases.

When a second carbonyl is replaced with a second pyridine (third row of **Scheme 1**), it was observed that for all ligand variations that 2Py23 is the most energetically unfavorable isomer (**Figure 2b**). This is due to steric hindrance between the two pyridines and the ligand. Surprisingly the most favorable isomers vary greatly depending on the ligand attached. In the case of L1 being attached, there are four energetically favorable isomers (1-2Py13, 1-2Py14, 1-2Py24 and 1-2Py34), there are two isomers for L2 (2-2Py12 and 2-2Py24), and one isomer for L3 (3-2Py13), L4 (4-2Py14) and L5 (5-2Py14) respectively. It is believed that the L1 complexes has 4 energetically favorable isomers due to the ligand having no added conjugation that would add steric hindrance, as well as the ligand having only minor twisting that would affect pyridine's ability to bind to certain positions. This twisting in ligand is why we see a drop in energetically favorable isomers for L2 and L3. In the case of L4 and L5 complexes with two pyridines, they are the most energetically favorable when both are placed in the axial position due to those positions causing the least amount of steric hindrance with the planar ligands.

If the two pyridines are bonded to form a bipyridine (**Figure 2c**) to add more rigidity to the complexes, as seen with the 2Py complexes, when the bipyridine is completely equatorial to the ligand (Bpy23) it is the least favorable isomer for all ligand types. For the 1-Bpy complexes the energetically favorable isomers follow along similarly with what was found for the 2Py isomers where 1-Bpy13 and 1-Bpy34 are energetically favorable with 1-Bpy24 being just out of K_T, the 2-Bpy and 3-Bpy complexes also have the same isomer energetically favorable as their 2Py versions. While the 4-Bpy and 5-Bpy complexes have a different energetically favorable isomer due to bipyridine not being able to attach in both axial positions like 4-2Py and 5-2Py were able to. They instead follow with what would be the next energetically favorable isomers for the 2Py cases, 4-Bpy24 and 5-Bpy24 respectively. The 4-Bpy complexes also have the 4-Bpy12 isomer being energetically favorable, as it is the mirror image of the 4-Bpy24 complex due to the planarity of L4. This is not the case for the 5-

Bpy complexes due to the slight bending caused to the L5 ligand where the conjugation was added, causing the two isomers to not be identical energetically.

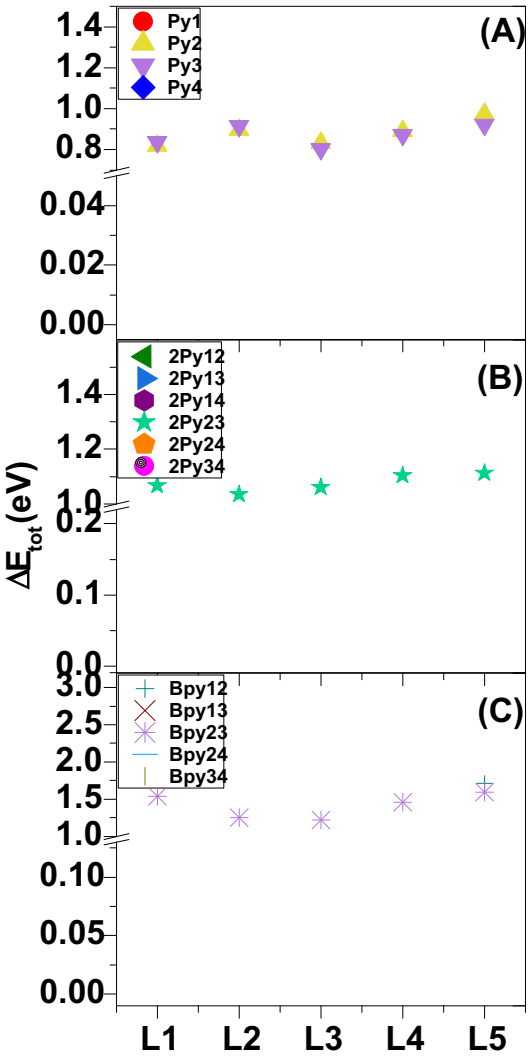


Figure 2 : Shows the difference in total energy of all isomers for Py (a), 2Py (b), and bpy (c) for all ligand types. The grey dotted line shows the K_T energy (0.025 eV) at room temp. All energy differences found under the K_T line is considered to be energetically favorable isomers.

After obtaining the most energetically favorable isomers, we went on and compared the absorbance spectrum to those obtained with four carbonyls. There were a few cases where the energetically favorable isomers obtained the same absorbance spectra. In those cases, only one isomer is shown in the following figures for simplicity (see **Figure S5-S9** for

absorption spectra for all isomers). When we compare the favorable isomers to the carbonyl case for complexes with L1 (**Figure 3**), we can immediately see that when one pyridine is attached, we see a significant redshift in the first optically active peak (~150 nm) compared to complex 1 (**Figure 3a**), although the third state still makes up the optically active state. When the natural transition orbitals (NTO's) are compared for the first and third state (**Table 1**), they are all mainly metal to ligand charge transfer (MLCT) but complex 1-Py4 has an additional ligand to ligand charge transfer (LLCT) from the pyridine in the HOTO to L1 in the LUTO. This additional charge transfer caused by the replacement of a strong sigma donor (carbonyl group) with a weaker π-acceptor could be the cause for the significant redshift. In **Figure 3b** it can be seen when we add an addition pyridine (2Py), we see an even further redshift occurs as well as the first or second state becoming optically active depending on the isomer. When the NTO's are compared for the different isomers, it is still mostly made up of MLCT character where the density travels to L1 and not significantly onto the pyridines in the LUTO. There are some LLCT characters with one of the two pyridines seen but it is minimal in comparison to the MLCT. There is also a significant amount of d orbitals still present in the LUTO compared to when only one pyridine is attached, this finding could be the part of the reason why a further redshift is seen. When a bipyridine is attached (1-Bpy34 in **Figure 3c**), the first peak stays optically active but has a stronger oscillator strength compared to the 2Py version (1-2Py24). This increase in intensity is due to the increase amount of π-π^* interactions seen between the HOTO and LUTO orbitals (**Table1**) on both the bipyridine and on L1.

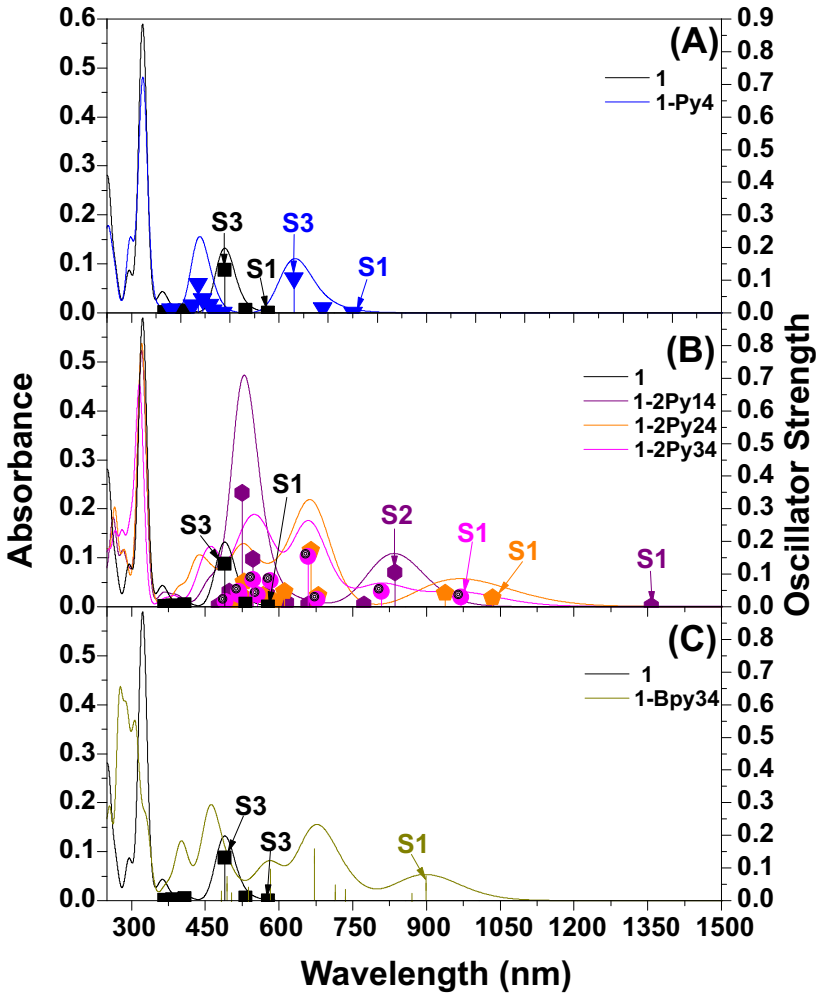
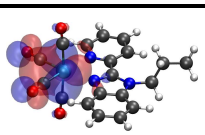
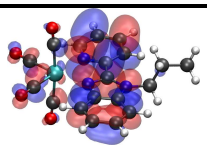
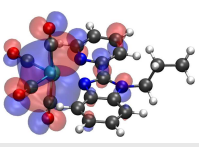
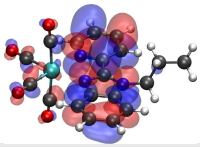
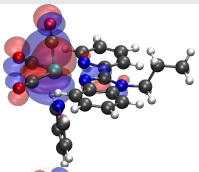
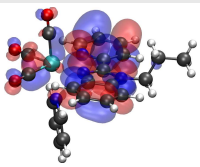
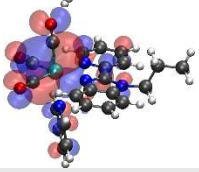
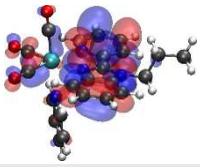
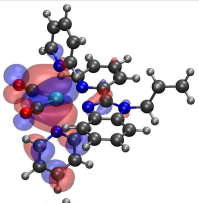
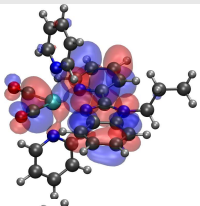
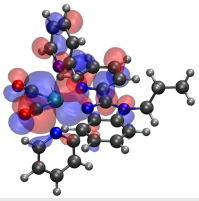
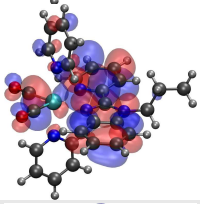
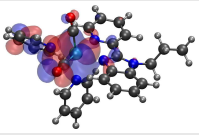
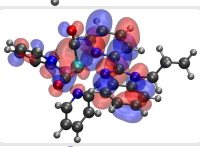
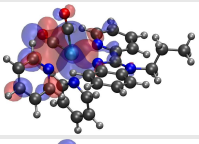
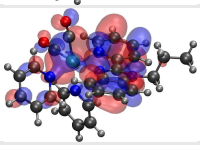
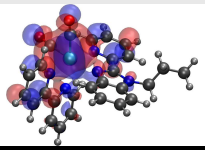
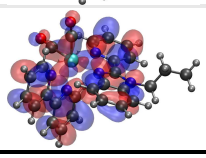


Figure 3: Shows the calculated absorbance spectra of the most energetically favorable isomers of all complexes with L1 for Py (a), 2Py (b), and Bpy (c).

Table 1: Hole and electron NTOs for the first optically active state of all energetically favorable complexes with ligand 1. All NTOs are Calculated using TDDFT on the ground state geometry with B3LYP functional and LANL2dz/6-31G* basis set with dichloromethane solvent using the CPCM method.

Complex	State/Wavelength/OS	Hole	Electron
1	**S_1** 578 nm *0.0001*		

	S_3 489 nm *0.1312*		
1-Py4	**S_1** 751 nm *0.0020*		
	S_3 631 nm *0.1071*		
1-2Py14	**S_1** 1358 nm *0.0013*		
	S_2 836 nm *0.1057*		
1-2Py24	**S_1** 1035 nm *0.0269*		
1-2Py34	**S_1** 971 nm *0.0290*		
1-Bpy34	**S_1** 899 nm *0.0528*		

Similar trends can be seen in **Figure 4** for the energetically favorable isomers for complexes containing L3, L4 and L5 (**Figure 4a, b**, and **c** respectively). In the case of complexes containing L3, we see similar trends with the first state becoming optically active when there are two pyridines or a bipyridine attached (3-2Py13 and 3-Bpy13). These states are also mainly MLCT with minimal LLCT in the cases of the isomers with pyridines and bipyridines (**Table 2**) where the charge transfers seem to be mainly to L3 instead of being split equally between L3 and the pyridines and bipyridine. This changes with L4 and L5 complexes particularly for the Bpy complexes (4-Bpy12 and 5-Bpy24 respectively). For

these complexes the MLCT is evenly distributed between the bipyridine and ligand which could be aiding in the intensity of the first peak. The L4 and L5 complexes also have significant π-π^* interactions that are causing the intensity of the first peak to be significantly higher than those complexes with the imidazole ligands attached.

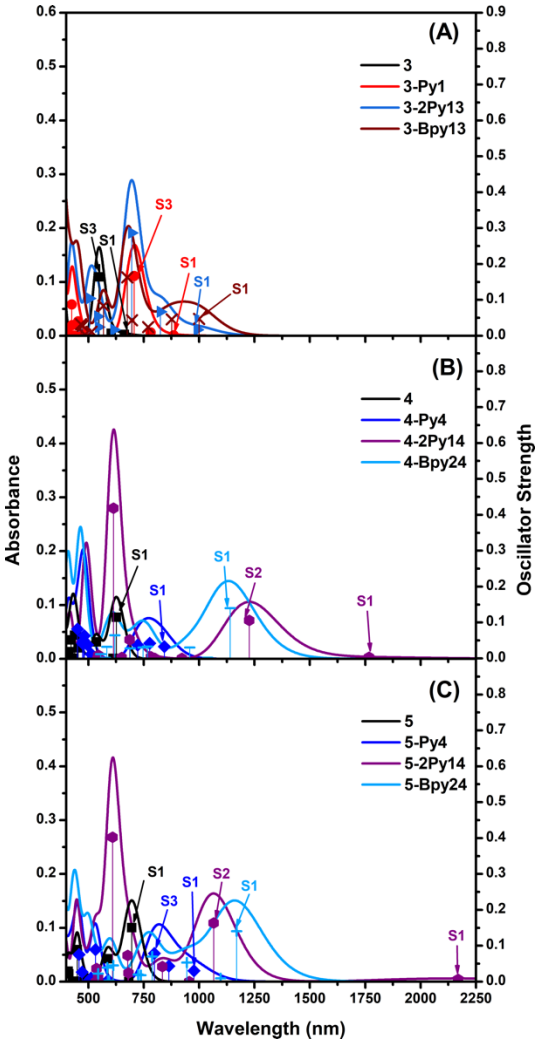
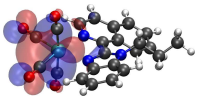
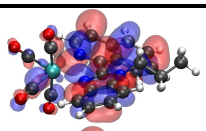
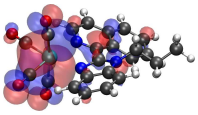
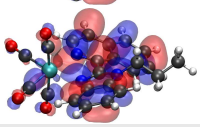
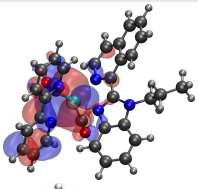
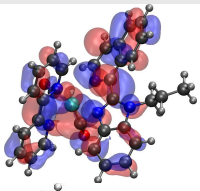
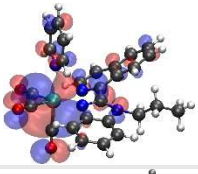
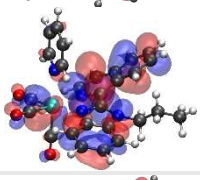
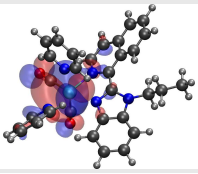
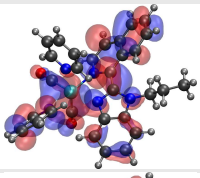
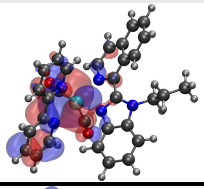
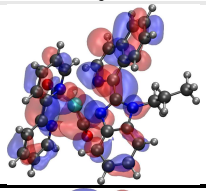
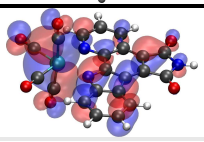
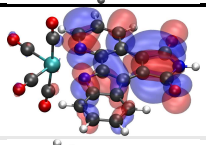
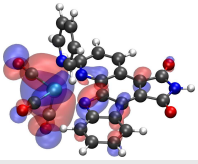
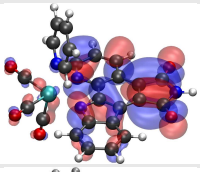
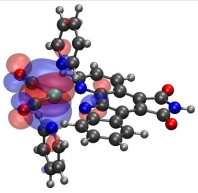
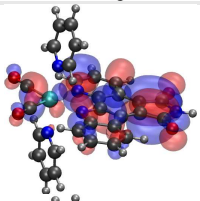
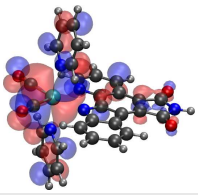
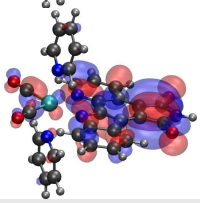
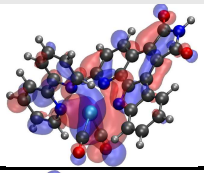
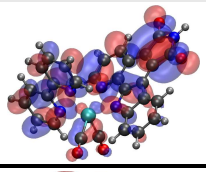
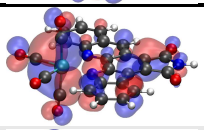
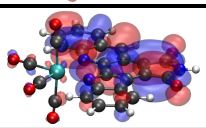
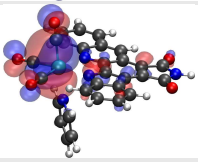
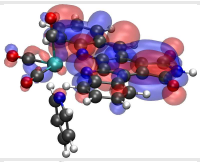
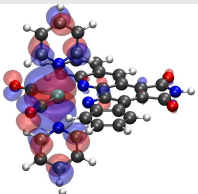
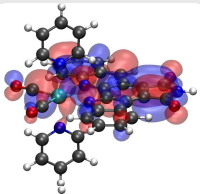
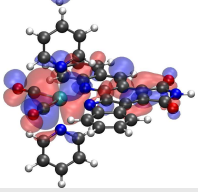
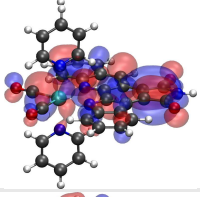
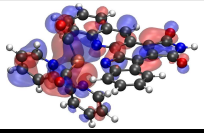
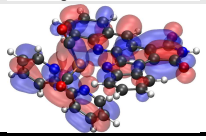


Figure 4: Shows the calculated absorbance spectra of the most energetically favorable isomers of all complexes with L3 (a), L4(b) and L5(c).

Table 2: Hole and electron NTOs for the first optically active state of all energetically favorable complexes for ligands 3, 4, and 5. All NTOs are Calculated using TDDFT on the ground state geometry with B3LYP functional and LANL2dz/6-31G* basis set with dichloromethane solvent using the CPCM method.

Complex	State/Wavelength/OS	Hole	Electron
3	**S_1** 663 nm *0.0039*		
	S_3 548 nm *0.1638*		
3-Py1	**S_1** 886 nm *0.0014*		
	S_3 707 nm *0.1663*		
3-2Py13	**S_1** 991 nm *0.0165*		
3-Bpy13	**S_1** 1000 nm *0.0470*		
4	**S_1** 626 nm *0.1148*		
4-Py1	**S_1** 845 nm *0.0336*		
4-2Py14	**S_1** 1768 nm *0.0029*		
	S_2 1226 nm *0.1058*		

4-Bpy12	**S_1** 1139 nm *0.1410*		
5	**S_1** 696 nm *0.1506*		
5-Py4	**S_1** 976 nm *0.0302*		
5-2Py14	**S_1** 2169 nm *0.0060*		
	S_2 1066 nm *0.1635*		
5-Bpy24	**S_1** 1169 nm *0.1408*		

Due to tungsten being a heavy metal there is a significant chance that these trends could be affected by spin orbit coupling contributions. Because of this SOC-TD-DFT was computed to see if there is mixing between singlet and triplet states that could affect the orbitals and overall shape of the absorption spectra for these complexes. When looking into the effect of SOC on the absorption spectra for L1 complexes (**Figure S11**), there are no significant changes in the overall look of the spectra besides slight shifting and broadening caused by the difference in basis set and number of states (see methods). When the molecular orbitals (MO's) that make up the SOC states are looked at (**Table S6**), complex 1 is pure singlet with no mixing with triplet states. This is also seen to be the case for complex 2 and 3 (**Table S7** and **Table S8** respectively). When a pyridine is added however, we see a slight mixing with the T_3 state (~4%) in the first peak although we don't see a significant difference in the MO's compared to the TD-DFT NTO's. When a second pyridine is attached (2Py) the amount of mixing between triplet and singlet states increases as more conjugation is added to the complexes, with 1-2Py being between 6 and 9% triplet depending on the isomer. For 1-Bpy34 a splitting of the first peak can be seen for SOC-TD-DFT where the state at 1015nm is made up of 11% singlet (S_1) and 83% triplet (T_3) while the state at 936 nm is 41% singlet (S_1) and 44% triplet (T_4). Similar trends can be seen for L2 (**Figure S12** and **Table S7**) and L3 (**Figure S13a** and **Table S8**) complexes. Overall for the imidazole complexes, it is seen that one pyridine attached (Py) has a small amount of

mixing, two pyridines (2Py) have slightly more mixing while bipyridine's peak is made up of multiple states that have a significant amount of mixing. The MO's for these states all look significantly similar to the NTO's from TD-DFT calculations of those states, showing that the overall charge transfers were not affected. This shows that for tungsten complexes with imidazole ligands, that SOC mixing increases as conjugation and rigidity increases. This does not seem to be the case when pyridocarbazole-type ligands (L4 and L5) are used. In this case although the spectra don't significantly change with SOC-TD-DFT (**Figure S13b** and **Figure S13c** respectively), complex 4 and 5 have a significant amount of triplet mixing in the first peak (**Table S9** and **Table S10** respectively). This increase in mixing could be due to the rigidity of the pyridocarbazole-type ligands in comparison to the slightly twisted imidazole ligands (L1, L2, and L3). The amount of mixing significantly decreases however when pyridine and bipyridines are attached. This was a surprising result that will need to be investigated further in the future.

In summary, coordinated complexes have been of great interest recently due to their wide range of properties that can be used for applications in fields such as photocatalysis, photovoltaics, and photodynamic therapy (PDT). Currently there is a need to find more earth abundant complexes that are more sustainable than current Ir(III), Ru(II), and Os(II) complexes. In this work we looked into the optical properties of W(0) carbonyl complexes with either imidazole (L1, L2, and L3) or pyridocarbazole-type ligands (L4 and L5) and found that replacing the carbonyls with one pyridine (Py), two pyridines (2Py) or a bipyridine (Bpy) would significantly redshift the first peak of the absorption spectra as far as 1250 nm in some cases. It was also found that this addition causes the first state to become optically active, when 2Py or Bpy are attached, which could make these complexes be of more interest in applications such as photodynamic therapy and solar cells due to increase ability to photoluminest. With tungsten being a heavy metal, it was found that the increase in bulkiness to the imidazole complexes through pyridine and bipyridine addition increased the mixing of singlet and triplet states in the first peak. This increase in mixing would be beneficial in applications that require intersystem crossing along with being in the NIR absorbance range. Overall, the imidazole ligands with one pyridine attached, along with complexes 4 and 5 show promise as photosensitizers for photodynamic therapy due to having an absorption in the therapeutic range (~650 nm-850nm) and having singlet and triplet mixing to aid in intersystem crossing. The other complexes studied in this work, although they are too red shifted for PDT, they could be of great interest in other applications such as photovoltaics or photocatalysis.

Methods:

Ground state properties of all complexes were calculated by optimizing the complexes using Gaussian 16 software[9,10] at the density functional theory[11] level. The B3LYP functional[12] was utilized and LANL2DZ[13] basis set was used for W(0) while 6-31g*[14] basis set was used for H, C, N and O atoms. The conductor polarizable continuum model (CPCM)[15] was utilized to simulate a dichloromethane (DCM) solvent environment to mimic experimental conditions.

The excited state properties were performed using linear-response time dependent DFT (TD-DFT)[16] as implemented in Gaussian 16 using the same basis sets, solvent model and functional used in ground state calculations. The absorption spectra were constructed from the first 100 computed excited states, each state was then dressed in the gaussian function using a linewidth of 0.2 eV to best represent thermal broadening seen commonly in experiments. The computed spectra for complexes 1, 2, and 3 were then compared to experimental data obtained by Dr. Wenfang Sun's group to confirm that our choice of functional compares well with experiment (Figure 1, see supporting information Figure 1-3 for functional comparison). Natural transition orbitals (NTO's)[17] were generated and visualized using VMD[18] from the transition density matrix that was obtained from TD-DFT calculations. The visualizations were given an isovalue of 0.02 to increase visibility of the orbitals but still allow insight into the electron hole pairs contributing to the first state and first optically active peaks that would be seen experimentally.

Spin orbit coupling was also taken into consideration when computing excited state properties(SOC-TD-DFT), as it is implemented in the ORCA 6.0.1 software[19]. These calculations utilized the B3LYP functional and CPCM model as before but used a mixed basis set of ZORA-def2-TZVP for H, N, C, and O atoms and SARC-ZORA-TZVP for W(0). This change in basis was required for SOC implementation due to ORCA not having SOC integrals for basis sets with electron core potentials (ECPs), causing a need for use of an all-electron basis. The absorption spectra were constructed using the first 100 singlet excited states (400 states with SOC), each state was then dressed in the gaussian function using a linewidth of 0.2 eV as before. Molecular orbitals (MO's) were generated and visualized using VMD with an isovalue of 0.02 to increase visibility of the orbitals but still allow insight into the contributing pairs for the first optically active peak that would be seen experimentally.

Acknowledgement:

Authors acknowledge support of SC0022239 by U.S. DOE.

References:

(1) Sun, X.; Shi, G.; Oas, V.; Gamage, K. D.; Talgatov, A.; Cameron, C. G.; Kilina, S.; McFarland, S. A.; Sun, W. Impact of Metal Center on Photophysics and In Vitro Photodynamic Therapeutic Activities of Ru(II)/Os(II)/Ir(III) Bis-Terpyridine Complexes Bearing Oligothienyl Substituents. **2025**, *64* (48), 23385. https://doi.org/https://doi.org/10.1021/acs.inorgchem.5c03296

(2) Wenger, O. S. Photoactive Complexes with Earth-Abundant Metals. *J. Am. Chem. Soc.* **2018**. https://doi.org/10.1021/jacs.8b08822

(3) Beaudelot, J.; Oger, S.; Peruško, S.; Phan, T.-A.; Teunens, T.; Moucheron, C.; Evano, G. Photoactive Copper Complexes: Properties and Applications. *Chem. Rev.* **2022**, *122* (22), 16365–16609. https://doi.org/10.1021/acs.chemrev.2c00033

(4) Yu, D.; To, W.-P.; Tong, G. S. M.; Wu, L.-L.; Chan, K.-T.; Du, L.; Phillips, D. L.; Liu, Y.; Che, C.-M. Luminescent Tungsten(VI) Complexes as Photocatalysts for Light-Driven C–C and C–B Bond Formation Reactions. *Chem. Sci.* **2020**, *11* (25), 6370–6382. https://doi.org/10.1039/D0SC01340D

(5) Lee, J. J.; Yap, C. P.; Chwee, T. S.; Fan, W. Y. Highly-Phosphorescent Tungsten(0) Carbonyl Pyridyl-Imidazole Complexes as Photosensitisers. *Dalton Trans.* **2017**. https://doi.org/10.1039/c7dt02397a

(6) Boden, P.; Di Martino-Fumo, P.; Bens, T.; Steiger, S.; Albold, U.; Niedner-Schatteburg, G.; Gerhards, M.; Sarkar, B. NIR-Emissive Chromium(0), Molybdenum(0), and Tungsten(0) Complexes in the Solid State at Room Temperature. *Chem. – Eur. J.* **2021**, *27* (51), 12959–12964. https://doi.org/10.1002/chem.202102208

(7) Fajardo, J.; Barth, A. T.; Morales, M.; Takase, M. K.; Winkler, J. R.; Gray, H. B. Photoredox Catalysis Mediated by Tungsten(0) Arylisocyanides. *J. Am. Chem. Soc.* **2021**, *143* (46), 19389–19398. https://doi.org/10.1021/jacs.1c07617

(8) Álvarez, D.; Menéndez, M. I.; López, R. Computational Design of Rhenium(I) Carbonyl Complexes for Anticancer Photodynamic Therapy. *Inorg. Chem.* **2022**, *61* (1), 439–455. https://doi.org/10.1021/acs.inorgchem.1c03130

(9) M. J. Frisch, G. W. Trucks, H. B. Schlegel, G. E. Scuseria, M. A. Robb, J. R. Cheeseman, G. Scalmani, V. Barone, G. A. Petersson, H. Nakatsuji, X. Li, M. Caricato, A. V. Marenich, J. Bloino, B. G. Janesko, R. Gomperts, B. Mennucci, H. P. Hratchian, J. V. Ortiz, A. F. Izmaylov, J. L. Sonnenberg, D. Williams-Young, F. Ding, F. Lipparini, F. Egidi, J. Goings, B. Peng, A. Petrone, T. Henderson, D. Ranasinghe, V. G. Zakrzewski, J. Gao, N. Rega, G. Zheng, W. Liang, M. Hada, M. Ehara, K. Toyota, R. Fukuda, J. Hasegawa, M. Ishida, T. Nakajima, Y. Honda, O. Kitao, H. Nakai, T. Vreven, K. Throssell, J. A. Montgomery, Jr., J. E. Peralta, F. Ogliaro, M. J. Bearpark, J. J. Heyd, E. N. Brothers, K. N. Kudin, V. N. Staroverov, T. A. Keith, R. Kobayashi, J. Normand, K. Raghavachari, A. P. Rendell, J. C. Burant, S. S. Iyengar, J. Tomasi, M. Cossi, J. M. Millam, M. Klene, C. Adamo, R. Cammi, J. W. Ochterski, R. L. Martin, K. Morokuma, O. Farkas, J. B. Foresman, and D. J. Fox. Gaussian 16, Revision C.01. **2016**.

(10) Roy Dennington, Todd A. Keith, and John M. Millam. GaussView, Version 6.1. **2016**.

(11) Kohn, W.; Sham, L. J. Self-Consistent Equations Including Exchange and Correlation Effects. *Phys. Rev.* **1965**, *140* (4A), A1133–A1138. https://doi.org/10.1103/PhysRev.140.A1133
(12) Becke, A. D. A New Mixing of Hartree–Fock and Local Density-Functional Theories. *J. Chem. Phys.* **1993**, *98* (2), 1372–1377. https://doi.org/10.1063/1.464304
(13) Hay, P. J.; Wadt, W. R. *Ab Initio* Effective Core Potentials for Molecular Calculations. Potentials for the Transition Metal Atoms Sc to Hg. *J. Chem. Phys.* **1985**, *82* (1), 270–283. https://doi.org/10.1063/1.448799
(14) Clark, T.; Chandrasekhar, J.; Spitznagel, G. W.; Schleyer, P. V. R. Efficient Diffuse Function-augmented Basis Sets for Anion Calculations. III. The 3-21+G Basis Set for First-row Elements, Li–F. *J. Comput. Chem.* **1983**. https://doi.org/10.1002/jcc.540040303
(15) Barone, V.; Cossi, M.; Tomasi, J. Geometry Optimization of Molecular Structures in Solution by the Polarizable Continuum Model. *J. Comput. Chem.* **1998**, *19* (4), 404–417. https://doi.org/10.1002/(SICI)1096-987X(199803)19:4%3C404::AID-JCC3%3E3.0.CO;2-W
(16) Casida, M. E.; Jamorski, C.; Casida, K. C.; Salahub, D. R. Molecular Excitation Energies to High-Lying Bound States from Time-Dependent Density-Functional Response Theory: Characterization and Correction of the Time-Dependent Local Density Approximation Ionization Threshold. *J. Chem. Phys.* **1998**, *108* (11), 4439–4449. https://doi.org/10.1063/1.475855
(17) Martin, R. L. Natural Transition Orbitals. *J. Chem. Phys.* **2003**, *118* (11), 4775–4777. https://doi.org/10.1063/1.1558471
(18) Humphrey, W.; Dalke, A.; Schulten, K. VMD: Visual Molecular Dynamics. *J. Mol. Graph.* **1996**. https://doi.org/10.1016/0263-7855(96)00018-5
(19) Neese, F. Software Update: The ORCA Program System—Version 5.0. *WIREs Comput. Mol. Sci.* **2022**, *12* (5), e1606. https://doi.org/10.1002/wcms.1606

Supplementary Files

This is a list of supplementary files associated with this preprint. Click to download.

- SITheroyWPaperV1.pdf